ADVANCING EARTH AND SPACE SCIENCES

Geophysical Research Letters

RESEARCH LETTER
10.1029/2023GL106410

Key Points:

- The CESM2 Atlantic meridional overturning circulation (AMOC) response to aerosols depends on if CMIP5 or CMIP6 emissions are applied
- Large interannual variability in CMIP6 emissions appears to enhance the interannual variability of north Atlantic turbulent heat fluxes
- This heat flux variability may drive a non-linear AMOC response to aerosols

Supporting Information:

Supporting Information may be found in the online version of this article.

Correspondence to:
M. R. Needham,
needham.michael@epa.gov

Citation:
Needham, M. R., Falter, D. D., & Randall, D. A. (2024). Changes in external forcings drive divergent AMOC responses across CESM generations. *Geophysical Research Letters*, *51*, e2023GL106410. https://doi.org/10.1029/2023GL106410

Received 14 SEP 2023
Accepted 13 FEB 2024

Changes in External Forcings Drive Divergent AMOC Responses Across CESM Generations

Michael R. Needham[1,2], Douglas D. Falter[3], and David A. Randall[1]

[1]Department of Atmospheric Science, Colorado State University, Fort Collins, CO, USA, [2]Now at United States Environmental Protection Agency, Lenexa, KS, USA, [3]Department of Geological and Atmospheric Sciences, Iowa State University, Ames, IA, USA

Abstract It has been suggested that the Atlantic meridional overturning circulation (AMOC) in many CMIP6 models is overly sensitive to anthropogenic aerosol forcing, and it has been proposed that this is due to the inclusion of aerosol indirect effects for the first time in many CMIP6 models. We analyze the AMOC response in a newly released ensemble of simulations performed with CESM2 forced by the CMIP5 input data sets (CESM2-CMIP5). This AMOC response is then compared to the CMIP5-generation CESM1 large ensemble (CESM1-LE) and the CMIP6-generation CESM2 large ensemble (CESM2-LE). A key conclusion, only made possible by this experimental setup, is that changes in aerosol-indirect effects cannot explain differences in AMOC response between CESM1-LE and CESM2-LE. Instead, we hypothesize that the difference is due to increased interannual variability of anthropogenic emissions. This forcing variability may act through a nonlinear relationship between the surface heat budget of the North Atlantic and the AMOC.

Plain Language Summary The Atlantic meridional overturning circulation (AMOC) is important for the wider climate because it transports a large amount of warm water northward away from the equator. The most recent generation of climate models disagree with the observed behavior of the AMOC over the twentieth century, and it has been suggested that this is due to the inclusion of aerosol-cloud interactions in many of the newest models. Here we look at model simulations of the AMOC in several configurations to show that the disagreement in the past AMOC behavior is instead primarily due to changes in the inputs given to the models, rather than to changes in the models themselves.

1. Introduction

The Atlantic meridional overturning circulation (AMOC; Buckley & Marshall, 2015; Lozier et al., 2019; Rahmstorf, 2002; Srokosz et al., 2021) is crucial in determining the local climate of the regions bordering the North Atlantic. It also plays a key role in the wider climate by accomplishing a significant portion of the necessary poleward energy transport determined by the top of atmosphere radiation balance (Chiang et al., 2008; Frierson et al., 2013; Marshall et al., 2013; Needham & Randall, 2023; Trenberth & Caron, 2001; Trenberth & Fasullo, 2017). The future behavior of the AMOC is of great interest because of its important role in the climate system: it has been identified as a potential climate "tipping point," (Broecker, 1987; Brovkin et al., 2021; Ditlevsen & Ditlevsen, 2023; Lenton et al., 2019), with the potential for a slowdown or collapse of the AMOC due to greenhouse gas-induced changes in the heat and salinity budgets of the north Atlantic.

Indirect observational and proxy-based estimates suggest that the AMOC has entered a period of decline, with a general slowdown relative to the pre-industrial era, particularly over the course of the twentieth century (Caesar et al., 2018, 2021; Rahmstorf et al., 2015; Thornalley et al., 2018), although this conclusion is not universally accepted (Worthington et al., 2021). In contrast, many models that participated in the most recent phase of the coupled model inter-comparison project (CMIP6; Eyring et al., 2016) predicted an *increase* in the strength of the AMOC over much of the twentieth century, likely due to the models' overly sensitive response to anthropogenic aerosol forcing (Hassan et al., 2021; Menary et al., 2020; Robson et al., 2022). These CMIP6 models also disagree with the older models of the CMIP5 generation, which more closely match observational AMOC estimates (Cheng et al., 2013; Menary et al., 2020).

The importance of the AMOC to the climate, and this significant model-observation disagreement motivate us to understand why models that participated in CMIP6 tend to overestimate the AMOC response to historic aerosol forcing. One hypothesis is that the first-time inclusion of aerosol-cloud interactions in many CMIP6 models

(Wang et al., 2021) led to excessive cooling of the northern relative to the southern hemisphere, which induced an increase in the strength of the AMOC (Menary et al., 2020). In this study we analyze a different hypothesis that has not yet been investigated to our knowledge: our goal is to quantify to what extent the change in external forcings from CMIP5 to CMIP6 contributes to the divergent AMOC responses of the CMIP5 and CMIP6 models. This hypothesis does not necessarily contradict the aerosol-cloud interaction hypothesis: both can contribute.

2. Data

We utilize three ensembles of coupled historical (1850– or 1920–present) simulations performed with the first (CESM1; Hurrell et al., 2013) or the second (CESM2; Danabasoglu et al., 2020) version of the Community Earth System Model at a nominal 1° horizontal atmospheric resolution. The first is a set of 35 simulations from the CESM1 large ensemble project using CMIP5 forcings (hereafter CESM1-LE; Kay et al., 2015); the second is 50 of the 100 simulations from the CESM2 large ensemble project using CMIP6 forcings (hereafter CESM2-LE; Rodgers et al., 2021); the third is 10 of the 15 simulations (only 10 simulations included all necessary fields at the time of analysis) performed using CESM2 but forced by the older CMIP5 inputs (hereafter CESM2-CMIP5; Holland et al., 2023). We use only the 50 members of the CESM2-LE which utilize smoothed biomass burning rather than the native CMIP6 biomass burning, because the later has been shown to lead to anomalous northern hemisphere warming toward the end of the historical period (Fasullo et al., 2022).

These three experimental configurations allow us to separate the different AMOC response to historic forcing into two components: the difference between CESM1-LE and CESM2-CMIP5 gives the impact of changing model versions with the external inputs held constant, while the difference between CESM2-CMIP5 an CESM2-LE gives the impact of changing the emissions from CMIP5 to CMIP6 in the same version of the model. Crucially, the CESM1 large ensemble employed the community atmosphere model version 5, which *does* include a representation of aerosol-cloud interactions (Hurrell et al., 2013; Kay et al., 2015), although the treatment of these interactions is different between CESM1 and CESM2 (Danabasoglu et al., 2020). Specifically, the atmospheric component of CESM2 utilizes an updated cloud microphysics scheme (MG2; Gettelman & Morrison, 2015) and an updated, four-mode aerosol model (MAM4; X. Liu et al., 2016).

All fields are ensemble means calculated from monthly mean model output. Annual mean timeseries anomalies are first computed by calculating monthly anomalies from the 20-year climatology defined as 1921–1940—the earliest period that is common to all simulations—and then calculating the average anomaly for each year. Yearly time series are then smoothed with an 11 years Gaussian filter with a standard deviation of 5 years.

3. AMOC Response to Historical Forcings

Panel a of Figure 1 shows the time series of the ensemble mean AMOC index anomaly for each of the three sets of simulations. The AMOC index is calculated as the maximum value of the overturning streamfunction in the Atlantic basin below a depth of 500 m (W. Liu et al., 2020). Shading shows the interquartile range among ensemble members. We use only the Eulerian component of the MOC, which is explicitly resolved by the model, although results are similar when the total (i.e., resolved plus parameterized) AMOC is analyzed (not shown).

The AMOC anomaly from the CESM2-LE (red curve) peaks in the later quarter of the twentieth century, which is consistent with other CMIP6 generation models (Menary et al., 2020; Robson et al., 2022). The AMOC anomaly from the CESM1-LE (blue curve) is typically negative over the historical period relative to 1921–1940, which in turn is consistent with other CMIP5 models. This establishes that CESM1 under CMIP5 and CESM2 under CMIP6 forcings are at least nominally representative of the wider CMIP5 and CMIP6 population of models discussed by Menary et al. (2020).

The AMOC anomaly from the CESM2-CMIP5 simulations (green curve) much more closely follows the CESM1-LE rather than the CESM2-LE curve from the beginning of the simulations in 1920 through to the 1980s. After about 1985 the CESM2-CMIP5 anomaly is essentially flat while both the CESM1-LE and CESM2-LE anomalies decrease at essentially the same rate. This result is the key finding of this study; it shows that the AMOC response in CESM2 is strongly dependent on the particular historical inputs (i.e., CMIP5 vs. CMIP6 emissions) to that model. It also establishes that the difference in AMOC response in CESM2-LE versus CESM1-LE cannot be explained solely by changes to the model.

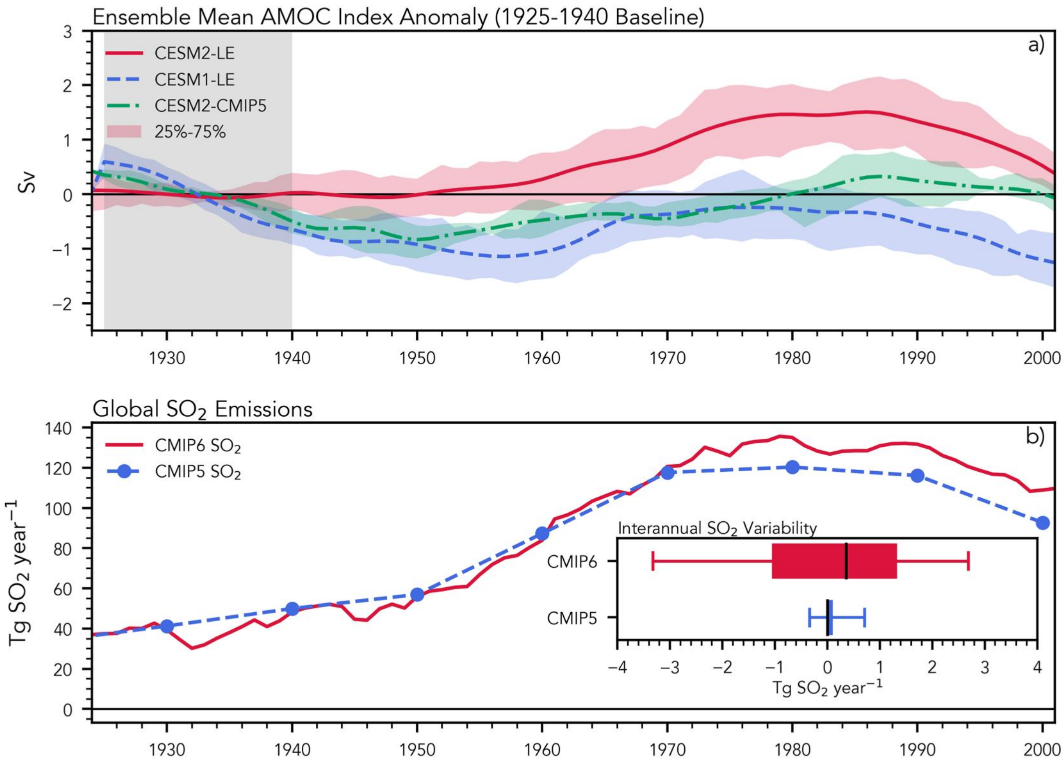

Figure 1. (a) Time series of the ensemble mean Atlantic meridional overturning circulation anomaly for three ensembles of climate simulations performed using the Comunity Earth System Model (see text for details of model configurations and forcings) (b) Global SO_2 emissions for CMIP5 and CMIP6. (Inset) Box plots of interannual SO_2 variability, defined as SO_2 minus smoothed SO_2 where the smoothing has been performed with the 11 years Gaussian filter. Whiskers show the 5th and 95th percentiles.

Previous studies have attributed the divergent AMOC responses of the CMIP5 and CMIP6 models to enhanced northern hemispheric cooling in CMIP6 models associated with the inclusion of aerosol indirect effects. However, as mentioned in the previous section, all three ensembles analyzed here employ atmospheric models (either CAM5 or CAM6) which include representations of aerosol-cloud interactions, yet we still observe a large difference in the AMOC response between the two ensembles forced with CMIP5 inputs and the CESM2-LE, which is forced by CMIP6 inputs. This result suggests that some property of the aerosol emissions is driving the divergent AMOC responses, and not the models' treatment of aerosol indirect effects.

The emissions of SO_2 are shown in panel b of Figure 1 and are analyzed as a bellwether for the wider group of aerosol precursors. On decadal time-scales the CMIP5 and CMIP6 emissions are largely similar, with a gradual increase throughout the twentieth century that accelerates after about 1950, peaks around 1980 and then begins to decline toward the end of the century. The magnitude of the emission rates is similar especially before 1970. The primary difference is that the CMIP5 emissions are given once a decade (blue points) and then interpolated to yearly timescales (blue dashed line), while the CMIP6 emissions are given once a year. Consequently, there is a higher degree of interannual variability in the CMIP6 SO_2 emissions. This is shown in the inset of Figure 1b, where the interannual variability is illustrated by showing the distribution of SO_2 emissions after the decadal-scale behavior has been removed (by subtracting the timeseries of the emissions after smoothing with the Gaussian filter). It is conceivable, then, that the higher temporal variability of these emissions in some way leads to the different AMOC response seen in the CESM2-LE and CESM2-CMIP5 ensembles. We return to this point in the discussion section.

4. Energy Budget of the North Atlantic

The AMOC is generally understood to be driven by a meridional pressure gradient between the tropics and higher latitudes. This pressure gradient is maintained by North Atlantic surface water which sinks when it becomes

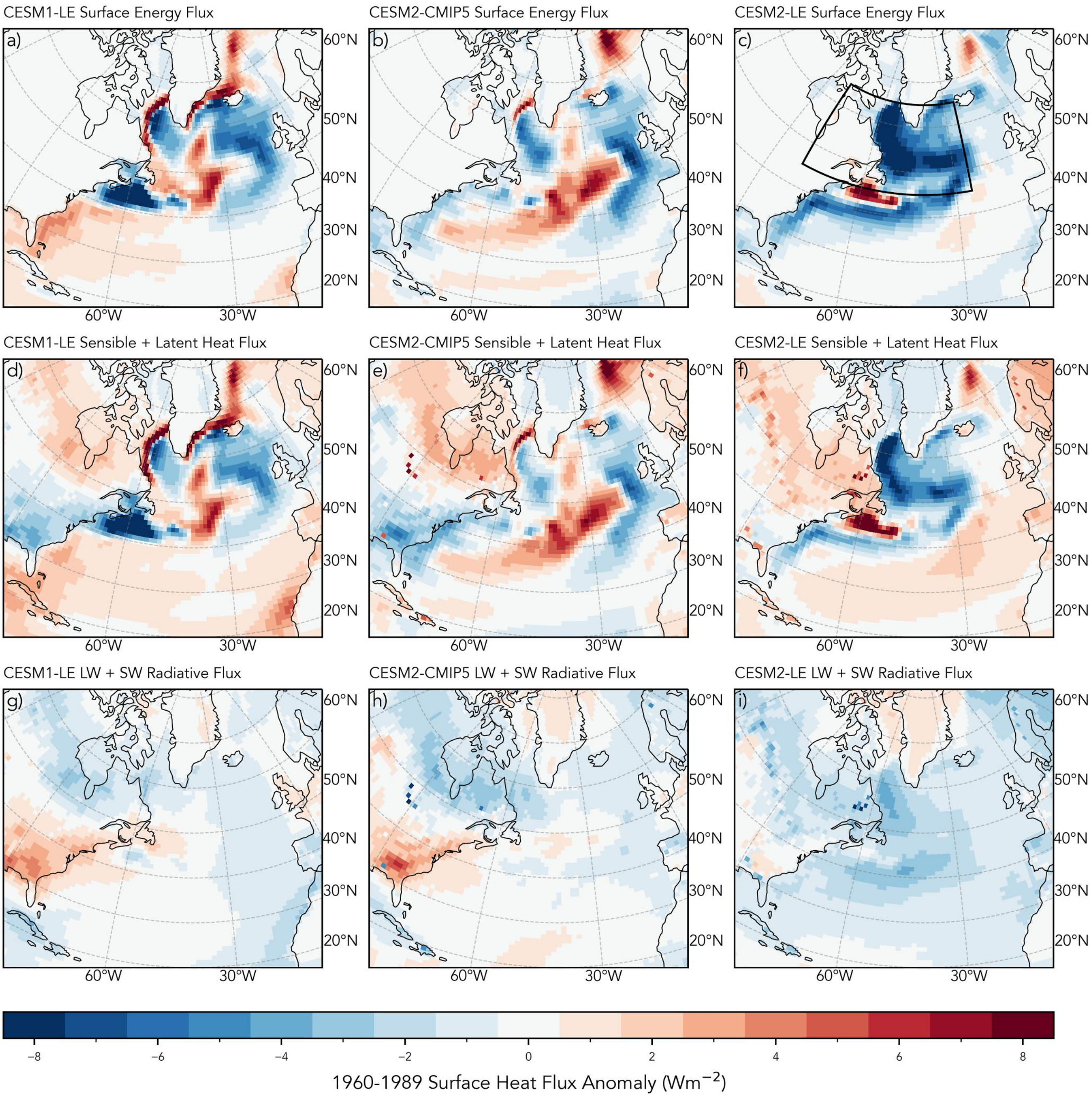

Figure 2. (a–c) Ensemble mean anomaly (1960–1989) in the net energy balance in the north Atlantic for the CESM1-LE, CESM2-CMIP5, and CESM2-LE ensembles (left, center, and right columns, respectively). (d–f) as in panels (a–c) but for the anomaly in the net sensible plus latent turbulent heat flux. (g–i) as in panels (a–c) but for the anomaly in the net longwave plus shortwave radiative flux at the surface. Negative (blue) values indicate an anomalous *heat loss* out of the ocean. The black boxed region in panel (c) indicates the region used for spatial averages in Figure 4, and is bounded by 80°W–25°W and 45°N–65°N.

anomalously cold and salty (i.e., through thermodynamic and haline effects). As discussed in the Supporting Information S1, we find that thermal fluxes are much more important in driving the AMOC than salinity-changing processes. Therefore, we next investigate the surface energy balance of the north Atlantic.

The top row of Figure 2 shows the average anomaly (1960–1989, relative to the 1921–1940 climatology) of the net surface energy flux over the subpolar north Atlantic (SPNA). It is immediately obvious that CESM2-LE has a much larger energy flux anomaly than either the CESM1-LE or the CESM2-CMIP5. The spatial pattern is also

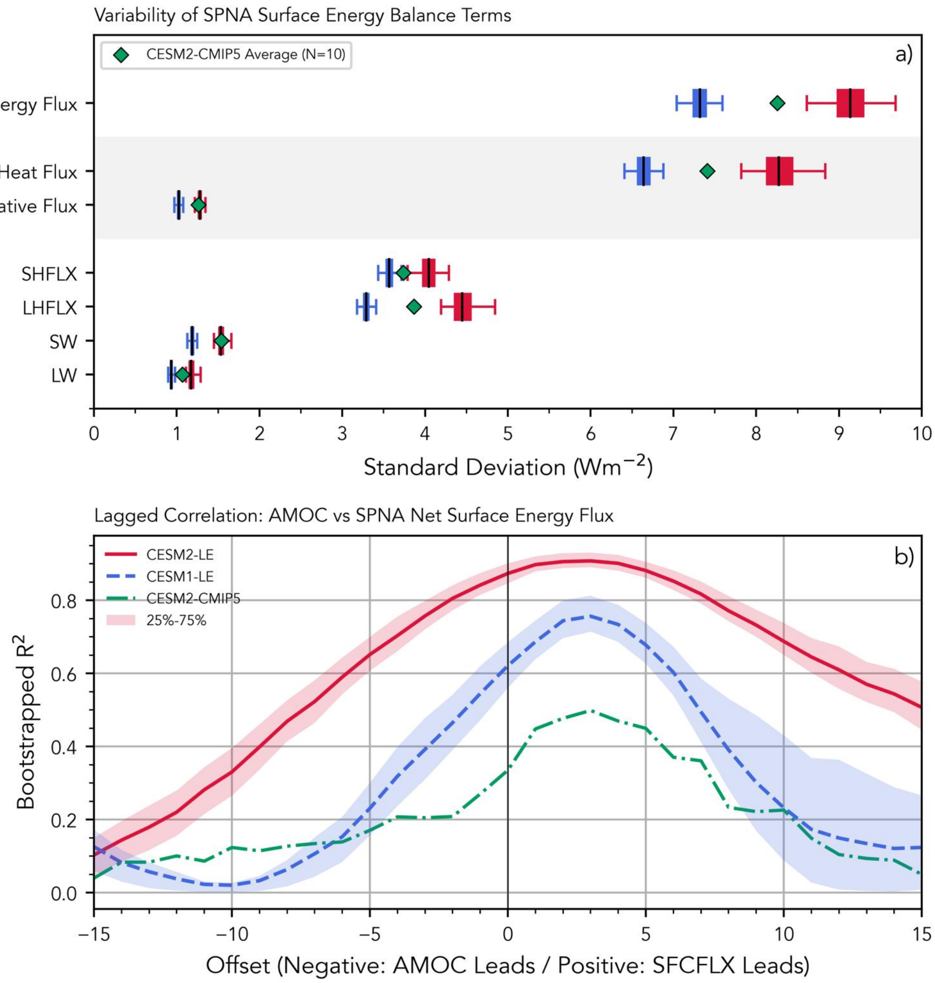

Figure 3. (a) Boxplots show the interannual variability (calculated using a bootstrapping method based on the mean of the yearly standard deviation; see text) of the terms of the subpolar north Atlantic (SPNA) heat budget between the CESM1-LE and CESM2-LE ensembles (blue and red, respectively), alongside the average standard deviation of the 10 CESM2-CMIP5 ensemble. Edges of boxes show the inter-quartile range, and whiskers indicate the 5th and 95th percentiles. Note the logarithmic scaling of the horizontal axis. (b) Time-lag correlation between Atlantic meridional overturning circulation (AMOC) anomaly and SPNA net surface heat flux computed using a bootstrapping method (again, see text for details). When the offset is positive (negative) AMOC lags (leads) SFCFLX.

different, with CESM2-LE producing negative anomalies across the entire north Atlantic, while CESM1-LE and CESM2-CMIP5 have a similar spatial structure with varying positive and negative anomalies. The middle row of the same figure shows the ensemble mean sensible plus latent turbulent heat flux. It is clear that the spatial structure of the surface heat flux anomaly (i.e., the top row) is primarily determined by turbulent surface fluxes, and not by surface radiation fluxes (i.e., the bottom row).

Similar to the SO_2 emissions in Figure 1, we find a greater degree of interannual variability in the CESM2-LE net surface energy flux than in either of the other ensembles, which is shown in Figure 3. Panel a shows the result of a bootstrapping approach to compare the ensemble mean of the 10 member CESM2-CMIP5 ensemble with that of the CESM1 and CESM2 ensembles for the standard deviation of the surface energy flux terms averaged over the subpolar North Atlantic (SPNA; shown as the outlined region in panel c of Figure 2). The distributions were calculated by randomly selecting 10 ensemble members out of the 50 (35) ensemble members from the CESM2 (CESM1) large ensemble, calculating the temporal standard deviation of the area-weighted annual mean timeseries, then calculating the average for the 10 ensemble members, and repeating this process 500 times. The standard deviations were calculated after removing the decadal scale behavior by calculating a smoothed timeseries using the same 11 years Gaussian filter and subtracting this from the full timeseries.

The SPNA energy flux in the CESM2-LE (red boxes) shows greater interannual variability than the other two ensembles. This is primarily due to the turbulent fluxes of latent and sensible heat with very little contribution from the radiative fluxes. From this experimental setup, the difference in interannual variability must be due to both changes in the model between CESM1 and CESM2, and to the different CMIP5 versus CMIP6 forcings. As the difference between the CESM2-CMIP5 and CESM2-LE ensembles is by definition due to changes in the forcings, this suggests the possibility that increased interannual variability in emissions may contribute to the increased interannual variability in the SPNA energy flux.

Even if this is shown to be the case, it must then be demonstrated that the SPNA energy flux in turn drives the AMOC response in the CESM2-LE, and not that the energy flux is in some way driven by the anomalous AMOC. One piece of evidence supporting this interpretation is shown in the bottom panel of Figure 3. Here, we have performed a time-lagged correlation analysis between these two variables. For a given offset (in years), we performed a similar bootstrapping method to that used in the top panel of the figure to generate the distribution of the 10-member sub-ensemble mean R^2 correlation for each of the large ensembles. We find the highest correlation when the surface energy flux anomaly leads the AMOC anomaly by about 2–3 years. This temporal relationship, combined with the canonical understanding of the AMOC as being driven by surface water that sinks in the north Atlantic after experiencing changes to its thermodynamic (i.e., through surface energy fluxes) and haline (i.e., through surface freshwater exchanges, which we show in the Supporting Information S1 to be much less important) properties suggests that the arrow of causality most likely points from the SPNA heat fluxes to the AMOC and not the other way around.

5. Discussion

As stated above, the primary result of this study is to show that the divergent AMOC responses to historical forcings between CESM1 and CESM2 is largely due to the changes in emissions between CMIP5 and CMIP6. It is beyond the scope of this study to definitively answer why the AMOC response in CESM2 is more sensitive to CMIP6 than CMIP5 forcings, however we briefly discuss one intriguing possibility here. As illustrated in panel b of Figure 1, the CMIP5 emissions estimates compiled by Lamarque et al. (2010) provided data at 10-year intervals: in contrast, the CMIP6 estimates compiled by Hoesly et al. (2018) are provided on an annual basis. We propose the hypothesis that the greater interannual variability of the CMIP6 forcings led to the stronger AMOC response in CESM2 purely because of the model's sensitivity to forcing variability. Our subsequent analysis (i.e., Figures 2 and 3) suggests that the interannual variability of emissions may be imprinted upon the surface energy flux, which appears to then drive the AMOC with a lag time of 2–4 years.

If confirmed, this hypothesis would be in line with a recent study by Fasullo et al. (2022). They showed that a discontinuity in the variability of biomass burning forcing—which arose from the inclusion of satellite observations of wildfire emissions from 1997 to 2014 but not before or after - led to “spurious warming” near the end of historical simulations performed with CESM2. In other words, the model was found to be noticeably sensitive to the temporal variability of biomass burning emissions. Similar results have been found in other studies (e.g., Yamaguchi et al., 2023 and references therein).

Does this principle of the influence of interannual forcing variability on coupled earth system models extend from the biomass burning emissions to other forcings such as anthropogenic emissions of SO_2? The top panels of Figure 4 show scatter plots of the AMOC anomly against the SPNA heat flux anomaly with no offset (panel a) and with an offset of 2 years (i.e., when the two timeseries displayed the highest degree of correlation in Figure 3). As with previous plots, these scatter plots were generated with a bootstrapping method where many sub-ensemble mean AMOC and SPNA heat flux anomalies are compared to one another.

There is a clear relationship between these two variables, but it does not appear to be a simple linear relationship. Specifically, when the surface heat flux anomaly is positive the AMOC response is also positive, while when the surface heat flux anomaly is negative the AMOC response remains near zero. Put another way, the slope of the best fit line between AMOC and SPNA heat flux is much steeper (1.225 Sv/Wm^{-2} vs. 0.025 Sv/Wm^{-2}) when the heat flux is positive than when it is negative. A piecewise regression using these two best fit lines against the full ensemble mean SPNA heat flux anomaly largely recreates the observed AMOC anomaly (panel c of Figure 4).

This indicates the possibility of a nonlinear “rectifier” effect (e.g., Denning et al., 1999) in which positive deviations of the SPNA heat flux have a much larger influence on the AMOC than negative deviations of the same

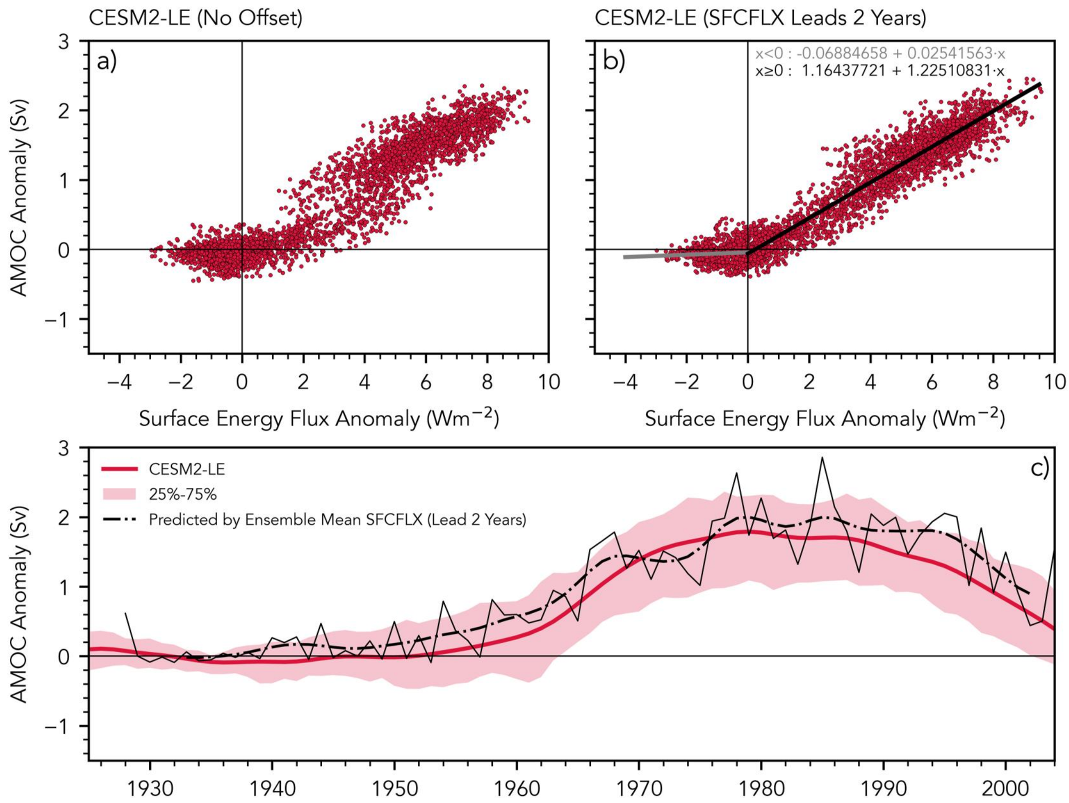

Figure 4. (a, b) Scatter plots of the CESM2-LE Atlantic meridional overturning circulation (AMOC) and SFCFLX anomalies with no offset (panel a) and with a 2 years negative offset (e.g., AMOC lags SFCFLX by 3 years, panel (b). Regression lines in panel (b) illustrate the non-linear "Rectifier" effect discussed in the text, where a positive anomaly in the SFCFLX leads to a larger anomaly in the AMOC compared to a negative anomaly of the same magnitude. (c) Comparison of the AMOC anomaly "predicted" by the non-linear regression shown in the top right panel (thin solid line; thick dash-dotted line smoothed with the same 11-year Gaussian filter) compared to the CESM2-LE ensemble mean AMOC anomaly.

magnitude. From the boxplots in Figure 3, CESM2-LE would tend to experience larger positive (as well as negative) deviations in the SPNA surface energy flux than either of the other ensembles, which may then be *rectified* onto the large positive AMOC anomaly seen in the top panel of Figure 1. We propose that the larger interannual variability in CMIP6 compared to CMIP5 forcings may be the root cause of this observed effect.

6. Conclusion

We have shown that the AMOC response in CESM2 is highly sensitive to the interannual-variability of external forcings. When run with CMIP6 forcings, CESM2 exhibits an increase in the strength of the AMOC from 1940 to 1985, consistent with many other CMIP6 models (Menary et al., 2020) and *inconsistent* with proxy reconstructions (Caesar et al., 2018, 2021; Rahmstorf et al., 2015; Thornalley et al., 2018). The fact that this AMOC anomaly is absent in both the CESM1-LE and when CESM2 is forced by the older CMIP5 inputs establishes that this difference cannot be explained by differences in the model but must be due in large part to a change in forcings from CMIP5 to CMIP6.

Combined with the time-lagged correlation analysis (Figure 3b), the fact that the spatially coherent heat flux anomaly seen in CESM2-LE (i.e., panel c of Figure 2) is largely absent in CESM1-LE indicates that the turbulent heat flux anomaly is a strong contributor to the different AMOC response between CESM1-LE and CESM2-LE, as in Hassan et al. (2021) and Robson et al. (2022); the fact that it is also absent in CESM2-CMIP5 indicates that the appearance of the heat flux anomaly is primarily due to a change in external forcings. Thus we conclude that the change in forcings between CMIP5 and CMIP6 played a key role in the divergent AMOC response between CESM1-LE and CESM2-LE. We then proposed the hypothesis that increased interannual variability of CMIP6 emissions may be the root cause of the AMOC disagreement. This hypothesis is in line with recent work highlighting the impact of interannual variability of biomass burning emissions on CESM2 (e.g., Fasullo et al., 2022; Yamaguchi et al., 2023) although this may be the first evidence of a similar effect in a different forcing (i.e., anthropogenic emissions vs. biomass burning). We also suggested that a nonlinear relationship between the SPNA heat flux and the AMOC (a "rectifier effect") may be the mechanism that connects the interannual variability of emissions to the AMOC.

A key limitation of this work is that we have analyzed only a single model. This particular experimental setup (in which each ensemble utilized an atmospheric model which includes aerosol indirect effects, although with different representations) makes it impossible to comment on the role of aerosol-cloud interactions on the AMOC across CMIP6 models except to say that those interactions did not play a role in the divergent AMOC response across CESM generations. However, we have no reason to believe that similar results would not be found if other models of the CMIP6 generation were forced by CMIP5 inputs. The stark differences between the AMOC response (Figure 1) and the heat flux anomaly over the north Atlantic (Figure 2 and panel a of Figure 3) in CESM2-CMIP5 and CESM2-LE would indicate that similar experiments comparing the response of CMIP6-generation models under CMIP5 inputs should be performed to better understand the impact of changing forcings. Such experiments could also help to better understand the role of the representation of aerosol-cloud interactions for those models that included those processes for the first time in CMIP6.

Data Availability Statement

Model output was accessed and analyzed via the Cheyenne System and Casper data analysis and visualization cluster (National Center for Atmospheric Research, 2019); figures were made using matplotlib (Hunter, 2007) and xarray (Hoyer & Hamman, 2017). The ensemble projects are described in Kay et al. (2015), Rodgers et al. (2021), and Holland et al. (2023).

Acknowledgments
We would like to thank the two anonymous reviewers for their thoughtful comments which helped to improve this manuscript. This work was supported by the National Oceanic and Atmospheric Administration through Grant NA19OAR4590155, and by the National Science Foundation through Grant AGS-1826643, both to the Colorado State University. Douglas D. Falter was supported by the National Science Foundation Research Experiences for Undergraduates Site in Earth System Science at Colorado State University under the cooperative agreement No. AGS-1950172.

References

Broecker, W. S. (1987). Unpleasant surprises in the greenhouse? https://doi.org/10.1038/328123a0

Brovkin, V., Brook, E., Williams, J. W., Bathiany, S., Lenton, T. M., Barton, M., et al. (2021). Past abrupt changes, tipping points and cascading impacts in the earth system. *Nature Geoscience*, *14*(8), 550–558. https://doi.org/10.1038/s41561-021-00790-5

Buckley, M. W., & Marshall, J. (2015). Observations, inferences, and mechanisms of the Atlantic meridional overturning circulation: A review. *Reviews of Geophysics*, *54*(1), 5–63. https://doi.org/10.1002/2015RG000493

Caesar, L., McCarthy, G. D., Thornalley, D. J. R., Cahill, N., & Rahmstorf, S. (2021). Current Atlantic meridional overturning circulation weakest in last millennium. *Nature Geoscience*, *14*(3), 118–120. https://doi.org/10.1038/s41561-021-00699-z

Caesar, L., Rahmstorf, S., Robinson, A., Feulner, G., & Saba, V. (2018). Observed fingerprint of a weakening Atlantic Ocean overturning circulation. *Nature*, *556*(7700), 191–196. https://doi.org/10.1038/s41586-018-0006-5

Cheng, W., Chiang, J. C. H., & Zhang, D. (2013). Atlantic meridional overturning circulation (AMOC) in CMIP5 models: RCP and historical simulations. *Journal of Climate*, *26*(18), 7187–7197. https://doi.org/10.1175/JCLI-D-12-00496.1

Chiang, J. C. H., Cheng, W., & Bitz, C. M. (2008). Fast teleconnections to the tropical Atlantic sector from Atlantic thermohaline adjustment. *Geophysical Research Letters*, *35*(7). https://doi.org/10.1029/2008gl033292

Danabasoglu, G., Lamarque, J.-F., Bacmeister, J., Bailey, D. A., Kushner, P. J., Larson, V. E., et al. (2020). The community earth system model version 2 (CESM2). *Journal of Advances in Modeling Earth Systems*, *12*(2). https://doi.org/10.1029/2019ms001916

Denning, A. S., Takahashi, T., & Friedlingstein, P. (1999). Can a strong atmospheric CO2 rectifier effect be reconciled with a "reasonable" carbon budget? *Tellus B: Chemical and Physical Meteorology*, *51*(2), 249–253. https://doi.org/10.1034/j.1600-0889.1999.t01-1-00010.x

Ditlevsen, P., & Ditlevsen, S. (2023). Warning of a forthcoming collapse of the Atlantic meridional overturning circulation. *Nature Communications*, *14*(1), 4254. https://doi.org/10.1038/s41467-023-39810-w

Eyring, V., Bony, S., Meehl, G. A., Senior, C. A., Stevens, B., Stouffer, R. J., & Taylor, K. E. (2016). Overview of the coupled model intercomparison project phase 6 (CMIP6) experimental design and organization. *Geoscientific Model Development*, *9*(5), 1937–1958. https://doi.org/10.5194/gmd-9-1937-2016

Fasullo, J. T., Lamarque, J.-F., Hannay, C., Rosenbloom, N., Tilmes, S., DeRepentigny, P., et al. (2022). Spurious late historical-era warming in CESM2 driven by prescribed biomass burning emissions. *Geophysical Research Letters*, *49*(2). https://doi.org/10.1029/2021gl097420

Frierson, D. M. W., Hwang, Y.-T., Fučkar, N. S., Seager, R., Kang, S. M., Donohoe, A., et al. (2013). Contribution of ocean overturning circulation to tropical rainfall peak in the northern hemisphere. *Nature Geoscience*, *6*(11), 940–944. https://doi.org/10.1038/ngeo1987

Gettelman, A., & Morrison, H. (2015). Advanced Two-Moment bulk microphysics for global models. Part I: Off-Line tests and comparison with other schemes. *Journal of Climate*, *28*(3), 1268–1287. https://doi.org/10.1175/JCLI-D-14-00102.1

Hassan, T., Allen, R. J., Liu, W., & Randles, C. A. (2021). Anthropogenic aerosol forcing of the Atlantic meridional overturning circulation and the associated mechanisms in CMIP6 models. *Atmospheric Chemistry and Physics*, *21*(8), 5821–5846. https://doi.org/10.5194/acp-21-5821-2021

Hoesly, R. M., Smith, S. J., Feng, L., Klimont, Z., Janssens-Maenhout, G., Pitkanen, T., et al. (2018). Historical (1750–2014) anthropogenic emissions of reactive gases and aerosols from the community emissions data system (CEDS). *Geoscientific Model Development*, *11*(1), 369–408. https://doi.org/10.5194/gmd-11-369-2018

Holland, M. M., Hannay, C., Fasullo, J., Jahn, A., Kay, J. E., Mills, M., et al. (2023). New model ensemble reveals how forcing uncertainty and model structure alter climate simulated across CMIP generations of the community earth system model [Dataset]. https://doi.org/10.5194/gmd-2023-125

Hoyer, S., & Hamman, J. J. (2017). xarray: N-D labeled arrays and datasets in python [Software]. Journal of Open Research Software, *5*, 304. https://doi.org/10.5334/jors.148

Hunter, J. D. (2007). Matplotlib: A 2d graphics environment [Software]. Computing in Science & Engineering, *9*(3), 90–95. https://doi.org/10.1109/MCSE.2007.55

Hurrell, J. W., Holland, M. M., Gent, P. R., Ghan, S., Kay, J. E., Kushner, P. J., et al. (2013). The community earth system model: A framework for collaborative research. *Bulletin of the American Meteorological Society*, *94*(9), 1339–1360. https://doi.org/10.1175/BAMS-D-12-00121.1

Kay, J. E., Deser, C., Phillips, A., Mai, A., Hannay, C., Strand, G., et al. (2015). The community earth system model (CESM) large ensemble project: A community resource for studying climate change in the presence of internal climate variability [Dataset]. Bulletin of the American Meteorological Society, *96*(8), 1333–1349. https://doi.org/10.1175/BAMS-D-13-00255.1

Lamarque, J.-F., Bond, T. C., Eyring, V., Granier, C., Heil, A., Klimont, Z., et al. (2010). Historical (1850–2000) gridded anthropogenic and biomass burning emissions of reactive gases and aerosols: Methodology and application. *Atmospheric Chemistry and Physics*, *10*(15), 7017–7039. https://doi.org/10.5194/acp-10-7017-2010

Lenton, T. M., Rockström, J., Gaffney, O., Rahmstorf, S., Richardson, K., Steffen, W., & Schellnhuber, H. J. (2019). Climate tipping points – Too risky to bet against. *Nature*, *575*(7784), 592–595. https://doi.org/10.1038/d41586-019-03595-0

Liu, W., Fedorov, A. V., Xie, S.-P., & Hu, S. (2020). Climate impacts of a weakened Atlantic meridional overturning circulation in a warming climate. *Science Advances*, *6*(26), eaaz4876. https://doi.org/10.1126/sciadv.aaz4876

Liu, X., Ma, P.-L., Wang, H., Tilmes, S., Singh, B., Easter, R. C., et al. (2016). Description and evaluation of a new four-mode version of the modal aerosol module (MAM4) within version 5.3 of the community atmosphere model. *Geoscientific Model Development*, *9*(2), 505–522. https://doi.org/10.5194/gmd-9-505-2016

Lozier, M. S., Li, F., Bacon, S., Bahr, F., Bower, A. S., Cunningham, S. A., et al. (2019). A sea change in our view of overturning in the subpolar north Atlantic. *Science*, *363*(6426), 516–521. https://doi.org/10.1126/science.aau6592

Marshall, J., Donohoe, A., Ferreira, D., & McGee, D. (2013). The ocean's role in setting the mean position of the Inter-Tropical convergence zone. *Climate Dynamics*, *42*(7), 1967–1979. https://doi.org/10.1007/s00382-013-1767-z

Menary, M. B., Robson, J., Allan, R. P., Booth, B. B. B., Cassou, C., Gastineau, G., et al. (2020). Aerosol-forced AMOC changes in CMIP6 historical simulations. *Geophysical Research Letters*, *47*(14). https://doi.org/10.1029/2020gl088166

National Center for Atmospheric Research. (2019). Computational and Information Systems Laboratory. HPE/SGI ICE XA System (University Community Computing).

Needham, M. R., & Randall, D. A. (2023). Anomalous northward energy transport due to anthropogenic aerosols during the 20th century. *Journal of Climate*, *1*(aop), 1–37. https://doi.org/10.1175/JCLI-D-22-0798.1

Rahmstorf, S. (2002). Ocean circulation and climate during the past 120,000 years. *Nature*, *419*(6903), 207–214. https://doi.org/10.1038/nature01090

Rahmstorf, S., Box, J. E., Feulner, G., Mann, M. E., Robinson, A., Rutherford, S., & Schaffernicht, E. J. (2015). Exceptional twentieth-century slowdown in Atlantic Ocean overturning circulation. *Nature Climate Change*, *5*(5), 475–480. https://doi.org/10.1038/nclimate2554

Robson, J., Menary, M. B., Sutton, R. T., Mecking, J., Gregory, J. M., Jones, C., et al. (2022). The role of anthropogenic aerosol forcing in the 1850–1985 strengthening of the AMOC in CMIP6 historical simulations. *Journal of Climate*, *35*(20), 3243–3263. https://doi.org/10.1175/JCLI-D-22-0124.1

Rodgers, K. B., Lee, S.-S., Rosenbloom, N., Timmermann, A., Danabasoglu, G., Deser, C., et al. (2021). Ubiquity of human-induced changes in climate variability [Dataset]. Earth System Dynamics, *12*(4), 1393–1411. https://doi.org/10.5194/esd-12-1393-2021

Srokosz, M., Danabasoglu, G., & Patterson, M. (2021). Atlantic meridional overturning circulation: Reviews of observational and modeling advances—An introduction. *J. Geophys. Res. C: Oceans*, *126*(1). https://doi.org/10.1029/2020jc016745

Thornalley, D. J. R., Oppo, D. W., Ortega, P., Robson, J. I., Brierley, C. M., Davis, R., et al. (2018). Anomalously weak Labrador Sea convection and Atlantic overturning during the past 150 years. *Nature*, *556*(7700), 227–230. https://doi.org/10.1038/s41586-018-0007-4

Trenberth, K. E., & Caron, J. M. (2001). Estimates of meridional atmosphere and ocean heat transports. *Journal of Climate*, *14*(16), 3433–3443. https://doi.org/10.1175/1520-0442(2001)014⟨3433:EOMAAO⟩2.0.CO;2

Trenberth, K. E., & Fasullo, J. T. (2017). Atlantic meridional heat transports computed from balancing earth's energy locally. *Geophysical Research Letters*, *44*(4), 1919–1927. https://doi.org/10.1002/2016GL072475

Wang, C., Soden, B. J., Yang, W., & Vecchi, G. A. (2021). Compensation between cloud feedback and aerosol-cloud interaction in CMIP6 models. *Geophysical Research Letters*, *48*(4). https://doi.org/10.1029/2020gl091024

Worthington, E. L., Moat, B. I., Smeed, D. A., Mecking, J. V., Marsh, R., & McCarthy, G. D. (2021). A 30-year reconstruction of the Atlantic meridional overturning circulation shows no decline. *Ocean Science*, *17*(1), 285–299. https://doi.org/10.5194/os-17-285-2021

Yamaguchi, R., Kim, J.-E., Rodgers, K. B., Stein, K., Timmermann, A., Lee, S.-S., et al. (2023). Persistent ocean anomalies as a response to northern hemisphere heating induced by biomass burning variability. *Journal of Climate*, *36*(23), 8225–8241. https://doi.org/10.1175/JCLI-D-23-0090.1